JOURNAL OF SOLID STATE CHEMISTRY 39, 15–21 (1981)

$Pb_4Fe_3O_8Cl$: Synthesis, Crystal Structure, and Thermal Expansion

J. PANNETIER[1]

Central Research and Development Department,[2] E. I. DuPont de Nemours and Co., Wilmington, Delaware 19898

AND P. BATAIL

Laboratoire Associé au CNRS n° 254, Laboratoire de Cristallochime, Université de Rennes-Beaulieu, Avenue du Général Leclerc, 35042 Rennes Cédex, France

Received November 26, 1979; in revised form January 28, 1981

$Pb_4Fe_3O_8X$ (X = Cl and/or Br) was prepared by solid state reaction. The structure of $Pb_4Fe_3O_8Cl$ was refined from X-ray single-crystal data in the centrosymmetric space group $P4/mmm$ (a = 3.9097(2), c = 15.2873(17)); it can be described as an interlayering of incomplete perovskite-like sheets ($Pb_4Fe_3O_8$) with sheets of Cl. Fe(1) has a fivefold square pyramidal coordination while Fe(2) is in a regular octahedron of oxygen. Thermal expansion was measured from 25 to 500°C.

Introduction

Hematophanite, $Pb_4Fe_3O_8Cl$, is a rare mineral whose structure was first studied by R. C. Rouse (*1*, *2*). One of the interesting features of this compound is the unusual fivefold coordination of two-thirds of the iron atoms. However, Rouse's study was conducted on natural samples of unknown composition and his assignment of the noncentrosymmetric space group $P4mm$ (as opposed to $P4/mmm$) is not unambiguous. The present work was carried out to extend the chemistry of this unusual compound, restudy its crystal structure, and investigate its physical properties.

[1] On leave of absence from Laboratoire Associé au CNRS n° 254, Laboratoire de Chimie Minérale D, Université de Rennes-Beaulieu.

[2] Contribution No. 2691.

Experimental

Room temperature cell constants were obtained from Guinier-Hagg X-ray powder photographs by least-squares refinement (KCl internal standard). A platelet measuring 0.46 × 0.46 × 0.02 mm perpendicular to the (110), ($\bar{1}$10), and (001) faces, respectively, was used for data collection on an Enraf–Nonius CAD4 automatic diffractometer. Data ($0 < h$, $k < 10$, $0 < l < 26$) were collected by the $\omega - 2\theta$ scan method using monochromatized Mo$K\alpha$ radiation up to $\sin\theta/\lambda = 1.3$ Å^{-1}. The scan range was computed according to the formula $\Delta\theta = (0.9 + 0.2 \tan\theta)$ and was extended by 25% on each end of the scan range for background measurements. The scan rate, based on a fast prescan, was computed such that 10^4 counts were to be obtained, if possible, in a maximum allowed time of

0022-4596/81/100015-07$02.00/0

80 sec for each reflection. An aperture with a height of 4 mm and a variable width of (4.0 + 0.87 tan θ) mm was placed in the front of the scintillation counter at a distance of 173 mm from the crystal. The intensities of 3 standard reflections, measured after every 50 reflections showed no variation during the course of data collection. A total of 975 reflections were collected and corrected for Lorentz polarization and absorption effects. The transmission coefficients ranged between 0.004 and 0.466 based on a linear transmission coefficient of 761.3 cm^{-1}. The data were subsequently corrected for absorption using the program AGNOST (*3*). The validity of the absorption correction was tested on a set of equivalent reflections (symmetry-related *hkl* and ψ scan). After symmetry-related reflections were averaged, 365 independent reflections were judged to be observed by the criterion $F_0^2 > 2\sigma(F_0^2)$.

High-temperature X-ray powder data were recorded on a Compagnie Générale de Radiologie diffractometer using Gerard–Barret high-temperature equipment (*4*). For liquid nitrogen measurements, a low-temperature device developed by D. Louer (*5*) was used. At each temperature, the powder pattern was recorded in the range $2° \leq \theta \leq 65°$ (Cu$K\alpha$) and the unit-cell parameters obtained by least-squares refinement; these parameters were subsequently least-squares fitted by a polynomial; these polynomials fit the observations to better than two SD_e.

Synthesis

$Pb_4Fe_3O_8X$ (X = Cl and/or Br) is prepared according to the reaction shown in Eq. (1)

$$7\,PbO + 3Fe_2O_3 + PbX_2 \rightarrow 2Pb_4Fe_3O_8X. \quad (1)$$

This solid state reaction is carried out in a quartz tube sealed under vacuum or in a platinum crucible in air at 600°C. $Pb_4Fe_3O_8Cl$ melts congruently at 875°C and loses $PbCl_2$ above 900°C. Single crystals can be prepared by slow cooling of the liquid in a platinum crucible. The red powder is stable in air and not attacked by water or alkaline solutions. Electrical resistivity measured at 298°K on a single crystal, perpendicular to the c axis, is $\sim 10^7$ ohm/cm. No structural transformation or decomposition was observed up to 900°C and 58 kbar. $Pb_4Fe_3O_8Br$ decomposes at 735°C (7 PbO–$PbBr_2$ eutectic). It is unstable in water and quickly decomposes to Pb(OH)Br + Fe_2O_3. Single crystals could not be grown.

Both $Pb_4Fe_3O_8Cl$ and $Pb_4Fe_3O_8Br$ are magnetically ordered at room temperature (*14*). No transition is observed by DTA or DSC before the melting point. Their powder patterns can be indexed with a tetragonal unit cell (Tables I and II). $Pb_4Fe_3O_8Cl$ and $Pb_4Fe_3O_8Br$ form a complete solid solution (Fig. 1). $Pb_4Fe_3O_8F$ was never obtained as a pure phase, but always contaminated by one or two other phases (Pb_2OF_2,$Pb_2Fe_2O_5$). The purest sample gave the following unit cell parameters: a = 3.895(2) c = 14.834(6) Å. All attempts to prepare $Pb_4Fe_3O_8I$ or a solid solution of $Pb_4Fe_3O_8Br_{1-x}I_x$ were unsuccessful. More unexpected is the impossibility of even partially substituting Fe^{3+} or Pb^{2+} by other cations (Al^{3+}, Ga^{3+}, Rh^{3+}, Cr^{3+}, Mn^{3+}, Cd^{2+}, Bi^{3+}, K^+, . . .).

TABLE I

UNIT-CELL PARAMETERS (20°C) IN Å AND Å^3

Compound	a	c	V
$Pb_4Fe_3O_8Cl$	3.9097(2)	15.2873(17)	233.68(3)
$Pb_4Fe_3O_8Br$	3.9175(4)	15.5605(24)	238.81(5)

The SD_e are given in parentheses and refer to the last digit.

TABLE II

POWDER DIFFRACTION PATTERNS (T = 20°C)

	$Pb_4Fe_3O_8Cl$			$Pb_4Fe_3O_8Br$		
$h\ k\ l$	d_{obs}	d_{calc}	I	d_{obs}	d_{calc}	I
0 0 3	5.1004	5.0958	5	5.2101	5.1868	5
1 0 0	3.9079	3.9097	60	3.9197	3.9175	60
0 0 4	3.8193	3.8118	35	3.8876	3.8901	20
1 0 2	3.4830	3.4808	5	—	—	—
0 0 5	—	—	—	3.1128	3.1121	5
1 1 0	2.7641	2.7646	90	2.7650	2.7701	100
1 0 4	2.7336	2.7330	100		2.7604	
1 1 2	—	—	—	2.6089	2.6096	5
1 1 4	2.2394	2.2400	60	2.2564	2.2565	50
2 0 0	1.9548	1.9548	55	1.9585	1.9588	60
0 0 8	1.9107	1.9109	15	1.9446	1.9451	30
2 1 0	1.74815	1.74847	30	1.75059	1.75197	30
2 0 4	1.74019	1.74040	20		1.74950	
1 0 8	1.71659	1.71682	15	1.74261	1.74215	15
2 1 4	1.58999	1.58998	60	1.59700	1.59744	70
1 1 8	—	—	—	1.59195	1.59184	40
2 2 0	1.38228	1.38229	20	1.38539	1.38505	25
2 0 8	1.36649	1.36649	25	1.37992	1.38019	25
3 0 0	1.30297	1.30324	5	—	—	—
2 2 4	1.29948	1.29988	10	1.30479	1.30482	10
2 1 8	1.28960	1.28997	15	1.30161	1.30176	10
0 0 12	1.27457	1.27394	5	—	—	—
3 1 0	1.23628	1.23636	25	1.23837	1.23883	30
3 0 4	1.23372	1.23349	20		1.23796	
1 0 12	1.21136	1.21126	10	1.23152	1.23103	15
3 1 4	1.17656	1.17634	10	1.18121	1.18042	10
1 1 12	1.15767	1.15701	5	1.17424	1.17441	5
2 2 8	1.12034	1.11999	10	1.12904	1.12824	15

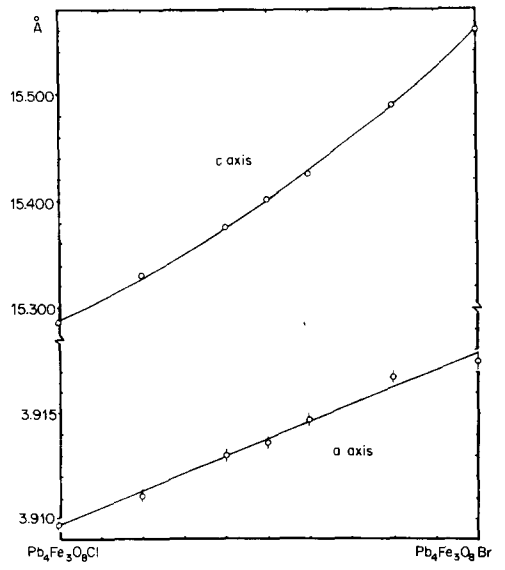

FIG. 1. $Pb_4Fe_3O_8Cl_{1-x}Br_x$: cell constants vs composition.

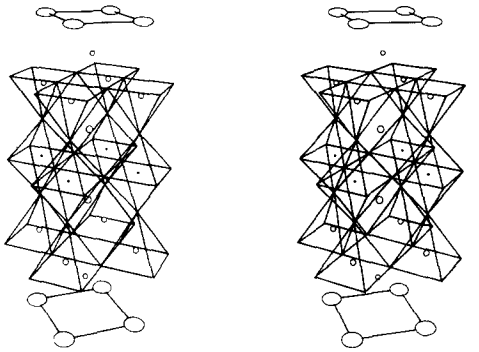

FIG. 2. Stereographic view of the $Pb_4Fe_3O_8Cl$ structure: the c axis runs vertically from bottom to top.

$Pb_4Fe_3O_8X$ (X = Cl, Br) seem to be the only example of that unusual structural type.

Crystal Structure

As noted in the introduction, the choice of noncentrosymmetric space group $P4mm$ by Rouse (*2*) does not seem justified; indeed, as easily seen by shifting the origin by ($\frac{1}{2}$, $\frac{1}{2}$, -0.121), Rouse's structure does not deviate significantly from a description in centrosymmetric space group $P4/mmm$. Moreover a second-harmonic-generation test on $Pb_4Fe_3O_8Cl$ powder was negative which favors the centric space group. Refinement with space group $P4/mmm$

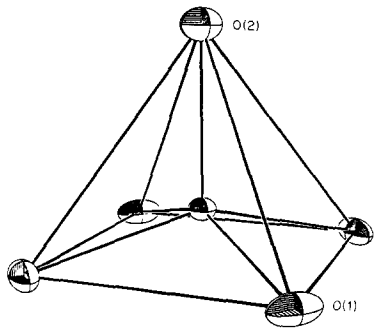

FIG. 3. Fe(1) coordination polyhedron. The ellipsoids are drawn at the 50% probability level.

TABLE III

ATOMIC COORDINATES AND THERMAL PARAMETERS[a]

Atom	Site	x	y	z	β_{11}	β_{22}	β_{33}	B_{eq}
Pb(1)	2*h*	½	½	0.1201(2)	0.0085(16)	β_{11}	0.0005(1)	.5
Pb(2)	2*h*	½	½	0.3802(3)	0.0167(25)	β_{11}	0.0011(1)	1.0
Fe(1)	2*g*	0	0	0.2440(11)	0.0112(46)	β_{11}	0.0006(4)	.5
Fe(2)	1*b*	0	0	½	0.0[b]	β_{11}	0.0009(4)	.2
O(1)	4*i*	0	½	0.212(1)	0.039(23)	0.011(13)	0.0010(7)	1.3
O(2)	2*g*	0	0	0.370(2)	0.026(12)	β_{11}	0.0008(9)	.5
O(3)	2*e*	0	½	½	0.22(14)	0.016(25)	0.0007(11)	4.8
Cl	1*a*	0	0	0	0.15(10)	β_{11}	0.0017(14)	6.5

[a] All β_{ij} $(i \neq j)$ are zero.

[b] Refinement of this thermal parameter converged to a negative value but with a large SD_e: $\beta_{11} = -.003$ (.005).

(starting from Rouse's coordinates transformed from *P4mm* to *P4/mmm*) quickly converged to $R = R_w = 0.061$ (24 refined parameters); the weighting scheme was that of McCandlisch *et al.* (*20*). Further refinement in space group *P4mm* did not improve the goodness of fit.

Refined atomic coordinates and anisotropic thermal parameters are given in Table III. The accuracy of the oxygen parameters is rather low, which can be attributed to the imprecision of the absorption correction. It is worth noting the high values of the thermal parameters of O(3) (which was previously obtained by Rouse as $B_{iso} = 4.0$ Å^2) and Cl (not refined in Rouse's structure). It is not clear whether these values have physical significance or only result from an imperfect absorption correction.

The qualitative features of the structure (Fig. 2) agree with Rouse's results. The structure can be described as a stacking of ($Pb_2Fe_3O_8$) and (Pb_2Cl) layers or, alternatively, as an interlayering of incomplete perovskitelike sheets ($Pb_4Fe_3O_8$) with a square bidimensional lattice of chlorine atoms. The presence of this chlorine layer with weaker Pb–Cl bonds explains the easy (001) cleavage of hematophanite crystals. This packing leads to the coordi-

TABLE IV

INTERATOMIC DISTANCES (Å)

Pb(1)–O(1)	2.411(13)	x4
Pb(1)–Cl	3.319(1)	x4
Pb(2)–O(1)	3.225(19)	x4
Pb(2)–O(2)	2.768(1)	x4
Pb(2)–O(3)	2.679(3)	x4
Fe(1)–O(1)	2.013(7)	x1
Fe(1)–O(2)	1.932(39)	x4
Fe(2)–O(2)	1.983(35)	x2
Fe(2)–O(3)	1.9548(1)	x4
O(2)–O(1)	3.107(33)	x4
O(2)–O(3)	2.784(25)	x4
O(1)–O(1)	2.7646(1)	x4
O(3)–O(3)	2.7646(1)	x4

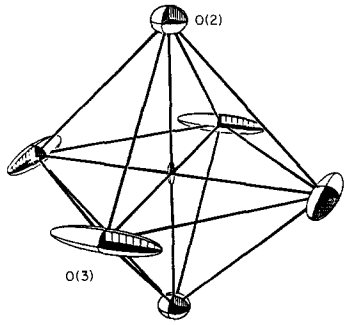

FIG. 4. Fe(2) coordination polyhedron.

TABLE V

Pb–O AND Pb–Cl DISTANCES (Å) IN CHLORIDES, OXIDES, AND OXYCHLORIDES

Compound	d(Pb–O)	d(Pb–Cl)	Ref.
$Pb_4Fe_3O_8Cl$: Pb1	2.41	3.319	this work
$Pb_4Fe_3O_8Cl$: Pb2	2.68, 3.22	—	this work
$PbBiO_2Cl$	2.45	3,25, 3.30	*7*
$PbSbO_2Cl$	2.542	3.137, 3.256	*8*
$Pb_2Cl_2CO_3$	2.37	2.95	*9*
Pb(OH)Cl	2.355, 2.441	3.112, 3.197, 3.441	*10*
$Pb_3O_2Cl_2$	2.19, 2.46	2.91, 3.53	*11*
$PbCl_2$	—	2.67, 3.29	*9*
PbFCl	—	3.25	*12*
Red PbO	2.31	—	*12*

nation polyhedra described below.

Fe(1) has a fivefold square pyramidal coordination (Fig. 3) and lies about 0.5 Å above the basal plane. The Fe–O distances of 2.01 and 1.93 Å (Table IV) are in good agreement with those calculated from Shannon's radii (*6*). The O(1)–Fe(1)–O(2) angle is 103.9(5)°. Fe(2) has an almost regular octahedral coordination (Fig. 4) with Fe–O distances slightly smaller than expected (1.995 Å). Pb(1) is in a distorted square antiprism of 4 O(1) and 4 Cl. The Pb–O distance is larger than in tetragonal PbO, but similar to the lead–oxygen distances observed in layered oxychlorides (Table V). Pb(2) has the usual 12-fold coordination (cuboctahedron) found in perovskite compounds. However, it is displaced by about 0.16 Å along the fourfold axis by the Pb(1)–Pb(2) electrostatic repulsion, giving an environment similar to that observed in $PbTiO_3$ (*9*).

Each chlorine atom occupies the center of a slightly flattened cube. The Cl–Cl distance of 3.91 Å is larger than that in $Pb_3O_2Cl_2$ (3.74 Å) (*11*). However, in $Pb_4Fe_3O_8Br$, the **a** cell constant of 3.9175 Å is twice the ionic radius of Br^- which suggests that the bromine ions are in contact. This could explain the nonexistence of $Pb_4Fe_3O_8I$ which would require a large

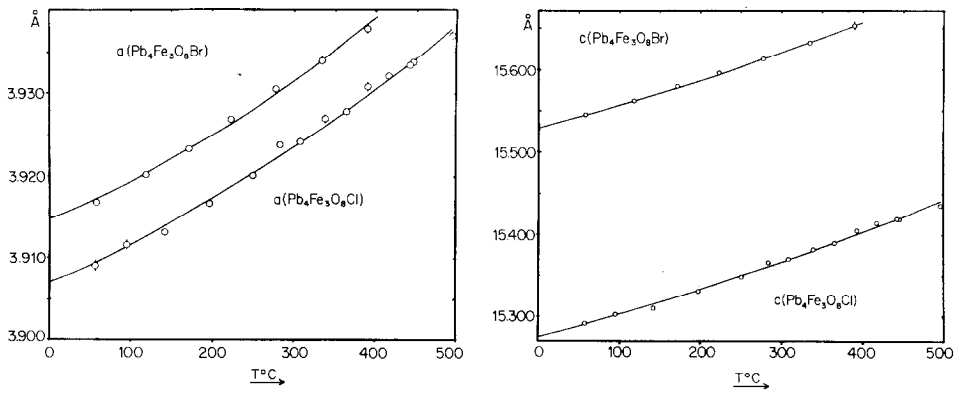

FIG. 5. $Pb_4Fe_3O_8X$ (X = Cl,Br): cell constants vs temperature.

TABLE VI

THERMAL EXPANSION: PARAMETERS OF THE POLYNOMIAL $a(T) = a_0 + a_1T + a_2T^2$ [a]

$Pb_4Fe_3O_8Cl$	$a_0 = 3.9071$	$a_1 = 0.443 \times 10^{-4}$	$a_2 = 0.36 \times 10^{-7}$
	$c_0 = 15.2761$	$c_1 = 0.261 \times 10^{-3}$	$c_2 = 0.14 \times 10^{-6}$
$Pb_4Fe_3O_8Br$	$a_0 = 3.9150$	$a_1 = 0.394 \times 10^{-4}$	$a_2 = 0.52 \times 10^{-7}$
	$c_0 = 15.5318$	$c_1 = 0.243 \times 10^{-3}$	$c_2 = 0.18 \times 10^{-6}$

[a] $a(T)$ in Å, T in °C.

a parameter (~4.40 Å), incompatible with the Fe–O distances in the ($Pb_4Fe_3O_8$) layer.

Thermal Expansion

Unit-cell parameters (Fig. 5) were measured from room temperature to 500°C and fitted to the polynomial $a(T) = a_0 + a_1T + a_2T^2$ (Table VI). Liquid nitrogen temperature parameters were also used to improve the polynomial fitting. The thermal expansion coefficients were calculated as

$$\alpha_a(T) = \frac{1}{a(T)}\left(\frac{da}{dt}\right)_T.$$

Since the crystals are tetragonal, the principal axes of the expansion tensors are along the crystallographic axis (Neumann's principle (*13*)). Above 400°C, we observed a sharp decrease of the c axis of $Pb_4Fe_3O_8Br$. This can be explained either by partial hydrolysis of the sample by moisture (Br–OH substitution) or by some exchange reaction with the internal KCl standard (Br–Cl substitution). These values were not used in the polynomial fit.

No thermal expansion anomaly is observed at the magnetic transition (330°C for $Pb_4Fe_3O_8Cl$ (*14*)). The thermal expansion of both $Pb_4Fe_3O_8Cl$ and $Pb_4Fe_3O_8Br$ is not very anisotropic. The α_c/α_a ratio is about 1.5 at room temperature and decreases at higher temperature, leading to a decreased asphericity index (*15*). This small ratio is somewhat unexpected since, in layer compounds, one usually observes a much higher expansion in the direction perpendicular to the layers, the result of different bond strengths along the directions parallel and perpendicular to the layers (*16*). For instance, in nadorite, $PbSbO_2Cl$, which has a similar layered structure (*8*), the α_c/α_a ratio is twice as large (*17*). Moreover, calculation of the electrostatic energy (*18*) as a function of the ($Pb_4Fe_3O_8$)–(Cl) sheet spacing shows a negligable variation, which means there is almost no electrostatic binding between the layers. However, calculation of the electrostatic fields (monopoles only) indicates high field values at the Pb(1) site ($E = 6.33$ V/Å). Since this field decreases rapidly as the interlayer spacing increases,[3] one suspects that the cohesive forces between the layers arise mainly from the polarization energy, $\alpha_{Pb}E^2$. It is noteworthy that the small thermal expansion of Red PbO has also been explained (*19*) by the high polarizability of Pb^{2+}.

Acknowledgments

We are indebted to Dr. A. W. Sleight for helpful discussions and to D. M. Richard and C. Poole for technical assistance. Dr. J. J. Mayerle (IBM, San

[3] A 1.4% increase of the c axis (keeping all Fe–O and Pb–O distances constant) leads to a 2.4% decrease of the electrostatic field at the Pb(1) site, but only to a 0.003% decrease of the Madelung energy.

Jose) is gratefully acknowledged for a critical reading of the manuscript.

References

1. R. C. ROUSE, *Amer. Mineral* **56,** 625 (1971).
2. R. C. ROUSE, *Mineral. Mag.* **39,** 49 (1973).
3. P. COPPENS, J. LEISEROWITZ, AND D. RABINOVICH, "AGNOST," Weizman Institute of Science, Rehovoth, Israel.
4. P. BARRET, N. GERARD, AND WATELLE-MARION, *Bull. Soc. Chim. Fr.* **8,** 3172 (1968).
5. D. LOUER, University of Rennes, private communication.
6. R. D. SHANNON, *Acta Crystallogr. Sect. A* **32,** 751 (1976).
7. M. GILBERT, *Arkiv Mineral. Geol.* **2,** 565 (1961).
8. G. GIUSEPPETI AND C. TADINI, *Period. Mineral.* **42,** 335 (1973).
9. R. W. G. WYCKOFF, "Crystal Structures," Vol. 1. Interscience, New York (1963).
10. C. VENETOPOULOS AND P. J. RENTZEPERIS, *Kristallogr.* **141,** 246 (1975).
11. H. VINCENT AND G. PERRAULT, *Bull. Soc. Fr. Crist. Mineral.* **94,** 323 (1971).
12. F. HULLIGER, *in* "Structure Chemistry of Layer-Type Phases" (F. Levy, Ed.), Reidel, Dordrecht (1976).
13. J. F. NYE, "Physical Properties of Crystals." Clarendon, Oxford (1969).
14. J. EMERY, A. CEREZE, AND F. VARRET, *J. Phys. Chem. Solids* **41,** 1035 (1980).
15. D. WEIGEL, P. GARNIER, AND J. F. BERAR, *C.R. Acad. Sci. Paris Ser. C* **283,** 305 (1976).
16. H. D. MEGAW, "Crystal Structures: A Working Approach," Saunders, Philadelphia (1973).
17. P. C. CHRISTIDIS AND P. J. RENTZEPERIS, *J. Appl. Crystallogr.* **10,** 486 (1977).
18. J. PANNETIER, unpublished computer program LATSUM for calculation of electrostatic energies, potentials and fields (1975).
19. M. A. BREDIG, *J. Chem. Phys.* **24**(5), 1037 (1956).
20. L. E. MCCANDLISCH, G. H. STOUT, AND L. C. ANDREWS, *Acta Crystallogr. Sect. A* **31,** 245 (1975).